

# Mechanistic Insights into the Pathogenesis of Proliferative and Nonproliferative Vitreomacular Traction



YOKO ITO, YUKI TAKATSUDO, PETER L. GEHLBACH, AND KEISUKE MORI

- **PURPOSE:** To describe the vitreoretinal interface in vitreomacular traction (VMT) by using novel optical coherence tomography (OCT) methods; wide-angle montage, and pseudomotion OCT imaging systems.
- **DESIGN:** Observational case series.
- **METHODS:** Wide-angle montage OCT images of horizontal and vertical scans through the fovea were acquired in 50 eyes of 46 consecutive patients with VMT. Baseline fundus scans were obtained. These were followed by scans acquired with an eye-tracking system performed immediately after vertical and horizontal eye movements. Three scans were then superimposed to compare changes in the contour and position of the posterior vitreous.
- **RESULTS:** The subjects were classified as VMT with (“proliferative”; 48.0%) and without (“nonproliferative”; 52.0%) thickened posterior vitreous. Epiretinal membrane was observed in 26.9% of nonproliferative and 95.8% of proliferative VMT eyes ( $P = 3.6 \times 10^{-7}$ ). No eye of proliferative and 57.7% of nonproliferative VMT eyes had wavy contoured posterior vitreous ( $P = 4.0 \times 10^{-6}$ ). None with proliferative VMT, but 91.7% of nonproliferative VMT eyes, showed motion induced changes of posterior vitreous following eye movement ( $P = 2.0 \times 10^{-8}$ ). The posterior vitreous detachment extended beyond the scanned area in 34.6% of nonproliferative and 8.3% of proliferative VMT eyes ( $P = .040$ ).
- **CONCLUSIONS:** By dynamically evaluating the vitreoretinal interface of patients with VMT, the static contraction forces of a thickened posterior vitreous at the macula are implicated in proliferative VMT. This contractile force is not strongly implicated in the majority of VMT eyes with nontaut and more mobile vitreous (nonproliferative VMT). VMT and its associated complica-

tions are determined by at least 2 different pathophysiological mechanisms. (Am J Ophthalmol 2022;238:1–9. © 2021 Elsevier Inc. All rights reserved.)

**A**BERRANT INTERACTIONS AT THE VITREORETINAL interface are recognized as an important pathological factor in a number of macular disorders including but not limited to cystoid macular edema, macular hole, epiretinal membrane (ERM), myopic traction maculopathy, and diabetic macular edema.<sup>1,2</sup> Abnormal vitreoretinal adhesion at the macula during posterior vitreous detachment (PVD) has been implicated and found to be integral in these disorders. The International Vitreomacular Traction Study Group has utilized optical coherence tomography (OCT)-based anatomic definitions of vitreomacular traction (VMT) to precisely describe the condition.<sup>3</sup> Various studies have further delineated fine anatomical alterations of the vitreoretinal interface by using OCT and have reported the characteristic findings that strongly implicate tractional force on the macula as one of the most important factors for development and progression of VMT.<sup>4–9</sup>

Previously, documented proliferative changes on the posterior cortical vitreous in VMT cases, have been described as “thickened posterior hyaloid”<sup>5,6</sup> or “hyper-reflective posterior hyaloid”<sup>7,8</sup> in OCT observations. This thick posterior vitreous is often contiguous with the ERM that becomes a backlining of the detached posterior vitreous. Histopathological studies revealed thick posterior vitreous and ERM in this type of VMT that also contained proliferative cell components including RPE cells, myofibroblasts, and fibrocytes.<sup>7,10</sup>

The findings of both histopathologic thickening and hyperreflectivity on OCT are uncommon in several conditions including traditionally called “idiopathic” macular holes with concurrent VMT. In our prior work using novel OCT imaging strategies and methods, macular holes are associated with a distinct morphological abnormality characterized by a thin and wavy rather than a thickened and taut posterior vitreous.<sup>11</sup> We also have reported on potential mechanistic findings at the vitreoretinal interface. A resulting fundamental observation concludes that dynamic posterior vitreous movements create anteroposterior tractional forces that act at the parafovea and induce macular hole initiation and progression.<sup>12</sup> It is also noteworthy

AJO.com Supplemental Material available at [AJO.com](https://ajoc.com).  
Accepted for publication November 29, 2021.

From the Department of Ophthalmology, International University of Health and Welfare, Nasu-shiobara, Tochigi, Japan (Y.I., Y.K., K.M.); The Wilmer Eye Institute, Johns Hopkins University School of Medicine, Baltimore, Maryland, USA (P.L.G.); Department of Ophthalmology, Saitama Medical University, Iruma, Saitama, Japan (K.M.)

Inquiries to Keisuke Mori, MD, PhD, Department of Ophthalmology, International University of Health and Welfare School of Medicine, 537-3 Iguchi, Nasu-Shiobara, Tochigi 329-2763, Japan.; e-mail: [cfh.htrai.arms2@gmail.com](mailto:cfh.htrai.arms2@gmail.com), [keisuke@iuhw.ac.jp](mailto:keisuke@iuhw.ac.jp)

**TABLE 1.** Demographic Data of Enrolled Subjects

		Nonproliferative VMT	Proliferative VMT	P Value
Age (years)	Mean $\pm$ SD (median)	69.5 $\pm$ 8.1 (70)	69.4 $\pm$ 10.4 (71)	.987 <sup>a</sup>
	Range	57–89	39–86	NA
Gender (M/F)	Cases	9/14	14/9	.238 <sup>b</sup>
	Eyes	9/17	15/9	.088 <sup>b</sup>

F = female; M = male; NA = not available; SD = standard deviation; VMT = vitreomacular traction .  
<sup>a</sup>t-test.  
<sup>b</sup>Fisher's exact test (CI: 95%).

thy that histopathological examination of macular hole demonstrated fibrocellular membrane fragments in only a minority of the surgical specimens obtained.<sup>13,14</sup>

Based on these findings, we focused on the proliferative changes at the vitreoretinal interface that may alter the tractional forces imparted by the fluid currents created by the mobile posterior vitreous. We subsequently considered VMT cases as either proliferative or nonproliferative, depending on the presence of a thickened posterior vitreous. To better understand the pathogenesis of VMT in each of these 2 test cases, we used previously reported OCT techniques to image patients with documented VMT. A montaged OCT imaging system that enables wide-field imaging from the macula to the equator<sup>11</sup> and a method that tracks the posterior cortical vitreous movement before and after prescribed ocular saccades, with an OCT eye-tracking system,<sup>12</sup> were used. Our results suggest that VMT-induced macular pathology is differentially predicted by OCT imaging, with eyes having nonproliferative type VMT having different fates than eyes with proliferative type VMT. These findings have a significant impact on mechanistic, pathophysiological, diagnostic, and therapeutic implications.

## METHODS

• **PATIENTS AND STUDY DESIGN:** This is a consecutive, observational case series. Fifty eyes of 46 patients with VMT were enrolled into this study (Table 1). The clinical diagnosis of VMT was determined by the OCT-based anatomic definition of International VMT group.<sup>3</sup> To analyze the incidence of associated findings, we included eyes with VMT and concurrent ERM and/or full-thickness macular hole. The investigation adhered to all of the tenets of the Declaration of Helsinki. This study was approved by the Institutional Review Board of the Saitama Medical University (approval no. 11-041-01) and the Ethics Committee of International University of Health and Welfare (approval no. 13-B-225). The composition of the subject population was 23 females and 23 males, ranging in age from 39 to 89 years old (mean, 69.5  $\pm$  9.2). All participants underwent indirect

ophthalmoscopic and slit-lamp biomicroscopic examination, refraction, and best-corrected visual acuity testing.

• **MONTAGED IMAGES AND GIF ANIMATIONS OF OCT:** The OCT examinations were carried out through a dilated pupil using commercially available spectral-domain OCT (Spectralis, Heidelberg Engineering) or swept-source OCT (DRI OCT Triton plus, Topcon). Standardized horizontal and vertical vitreoretinal sections through the fovea were collected for each subject. To obtain the maximum imaging depth into the vitreous and vitreoretinal interface, the retinochoroidal layers were set at the bottom of the image plane and the scans were focused on the vitreous. The planimetric image editing system was used to enhance visualization of the vitreous images.<sup>15–17</sup>

For the wider angled examination of the posterior vitreous and the vitreoretinal interface, OCT images were montaged. This technique permits observation from the macula to the periphery, approximately to the equator.<sup>11,12,18,19</sup> The montaged images were assembled by picture editing software, Photoshop (version 5.5, Adobe). The maximum width of vitreous attachment to the macula was measured on OCT images. The incidence of focal ( $\leq 1,500 \mu\text{m}$ ) or broad VMT ( $> 1,500 \mu\text{m}$ ),<sup>3,20</sup> and V-shaped (PVD with temporal and nasal detachment but persistent attachment at the fovea) or J-shaped VMT (an incomplete PVD with persistent foveal and nasal attachment but temporal detachment to the fovea)<sup>21,22</sup> was evaluated.

To examine the mobility of the posterior cortical vitreous during eye movement, the superimposed OCT images and their GIF format animations were created using Photoshop software. Specifically, after the OCT images were acquired in the static eye state (baseline), patients were asked to move their eyes up-and-down 3 times or right-and-left 3 times, just before OCT scanning, at which point a single scan of the same portion of the fundus was acquired using the OCT Eye Tracking System. The images of both the static and post ocular motion states were then reconstituted in Photoshop software to make a standardized overlaid OCT image, and a pseudoanimation GIF. Thirteen eyes were excluded from the superimposed OCT examination because the patient's consent was not obtained.

**TABLE 2.** Characteristic Findings of Optical Coherence Tomography Imaging

	Nonproliferative VMT	Proliferative VMT	P Value <sup>a</sup>
ERM	7/26 (26.9)	23/24 (95.8)	$3.6 \times 10^{-7}$
Macular hole	11/26 (42.3)	2/24 (8.3)	$9.2 \times 10^{-3}$
Wavy configuration of posterior vitreous	15/26 (57.7)	0/24 (0)	$4.0 \times 10^{-6}$
Fibrous anchor	0/26 (0)	23/24 (95.8)	$2.2 \times 10^{-13}$
PVD expansion beyond the scanned area	9/26 (34.6)	2/24 (8.3)	.040
Movement of posterior vitreous <sup>b</sup>	21/23 (91.7)	0/14 (0)	$2.0 \times 10^{-8}$
The width of vitreous attachment ( $\mu\text{m}$ , mean $\pm$ SD)	401.1 $\pm$ 462.2	2364.6 $\pm$ 2108.9	$1.0 \times 10^{-6}$
Focal/broad VMT	25/1	12/12	$2.3 \times 10^{-4}$
V-/J-shaped VMT	26/0	20/4	.046

Number of positive eyes/total eyes (%).

ERM = epiretinal membrane; PVD = posterior vitreous detachment; SD = standard deviation; VMT = vitreomacular traction.

<sup>a</sup>Fisher's exact test (CI: 95%), except the width of vitreous attachment (Mann-Whitney *U* test).

<sup>b</sup>Thirteen eyes (3 nonproliferative VMT; 10 proliferative VMT) were excluded from the superimposed OCT imaging analysis since the consent was not obtained.

• **STATISTICAL ANALYSIS:** The incidence of each phenotype was statistically analyzed using Fisher's exact test, *t* test, or Mann-Whitney *U* test. The results were considered to be statistically significant at a *P* value of less than .05. All analyses were performed using open-source software for statistical analysis, JASP (JASP Team, 2020 Version 0.14.1).

## RESULTS

• **THE OBSERVATIONS OF THE POSTERIOR VITREOUS AND THE MACULA IN PROLIFERATIVE AND NONPROLIFERATIVE VMT:** Of the 50 eyes examined, there were 24 eyes with proliferative VMT; the remaining 26 eyes had nonproliferative VMT. There was no significant difference in age/gender distribution between these 2 groups (Table 1). The incidence of concurrent ERM at the parafoveal area was high in eyes with proliferative VMT (23/24 eyes [95.8%]) and low in eyes with nonproliferative VMT (7/26 eyes [26.9%]) ( $P = 3.6 \times 10^{-7}$ ). Nonproliferative VMT showed focal and mild macular deformity with regard to the extent of foveal elevation, intrafoveal cysts and splitting of retinal layers, and was notably associated with full-thickness macular holes in 11 of 26 eyes (42.3%). There were only 2 eyes with macular hole in 24 eyes with proliferative VMT (8.3%) (Table 2) ( $P = 9.2 \times 10^{-3}$ ).

Eyes with proliferative VMT had a greater predisposition to broad vitreomacular attachment (mean. 2364.6  $\pm$  2108.9  $\mu\text{m}$ ) than eyes with nonproliferative VMT (401.1  $\pm$  462.2  $\mu\text{m}$ ) (Table 2) ( $P = 1.0 \times 10^{-6}$ ). Twelve of 24 eyes with proliferative VMT (50.0%) and 1 of 26 eyes with nonproliferative VMT (3.8%) were classified as having broad VMT (Table 2) ( $P = 2.3 \times 10^{-4}$ ). Four

eyes with proliferative VMT (16.7%) showed a J-shaped VMT and 20 eyes showed V-shaped VMT. All eyes with nonproliferative VMT showed V-shaped VMT (Table 2) ( $P = .046$ ).

In eyes with proliferative VMT, the posterior vitreous typically detached from the retina showing a taut convex (anterior protrusion) configuration (Figure 1). Thick posterior vitreous was seen to be broadly connected to ERM with multiple anchoring points over the macula (Figure 2). In contrast, in eyes with nonproliferative VMT the posterior vitreous was not taut but rather had a relaxed wavy-contoured posterior vitreous (15/26 eyes [57.7%]), suggestive of vitreous mobility (Figures 3 and 4, Table 2) ( $P = 4.0 \times 10^{-6}$ ). The presence of fibrous anchors on the retinal surface restricted PVD around the macular and paramacular regions in proliferative VMT eyes (23/24 eyes [95.8%]) (Figures 1 and 2), but no such anchors were seen in nonproliferative VMT eyes (Table 2) ( $P = 2.2 \times 10^{-13}$ ). The posterior cortical vitreous was detached beyond the observable image range, in at least 1 quadrant, in 9 of 26 eyes (34.6%) in nonproliferative VMT eyes (Figures 3 and 4). This was less common in proliferative VMT eyes (2/24 eyes [8.3%]) (Figures 1 and 2, Table 2) ( $P = .040$ ).

• **SUBSTANTIAL FLEXIBILITY OF THE POSTERIOR VITREOUS IN NONPROLIFERATIVE VMT WITH EYE MOVEMENT:** Imaging of the posterior vitreous before and after eye movement revealed that no eye with proliferative VMT showed changes in the configuration or position of the posterior vitreous (0/14 eyes), which was continuously taut, maintaining a nonwavy, convex contour (Figure 1D and E, Supplemental Data/Video 1). In contrast, 21 of 23 eyes (91.7%) with nonproliferative VMT showed changes in posterior

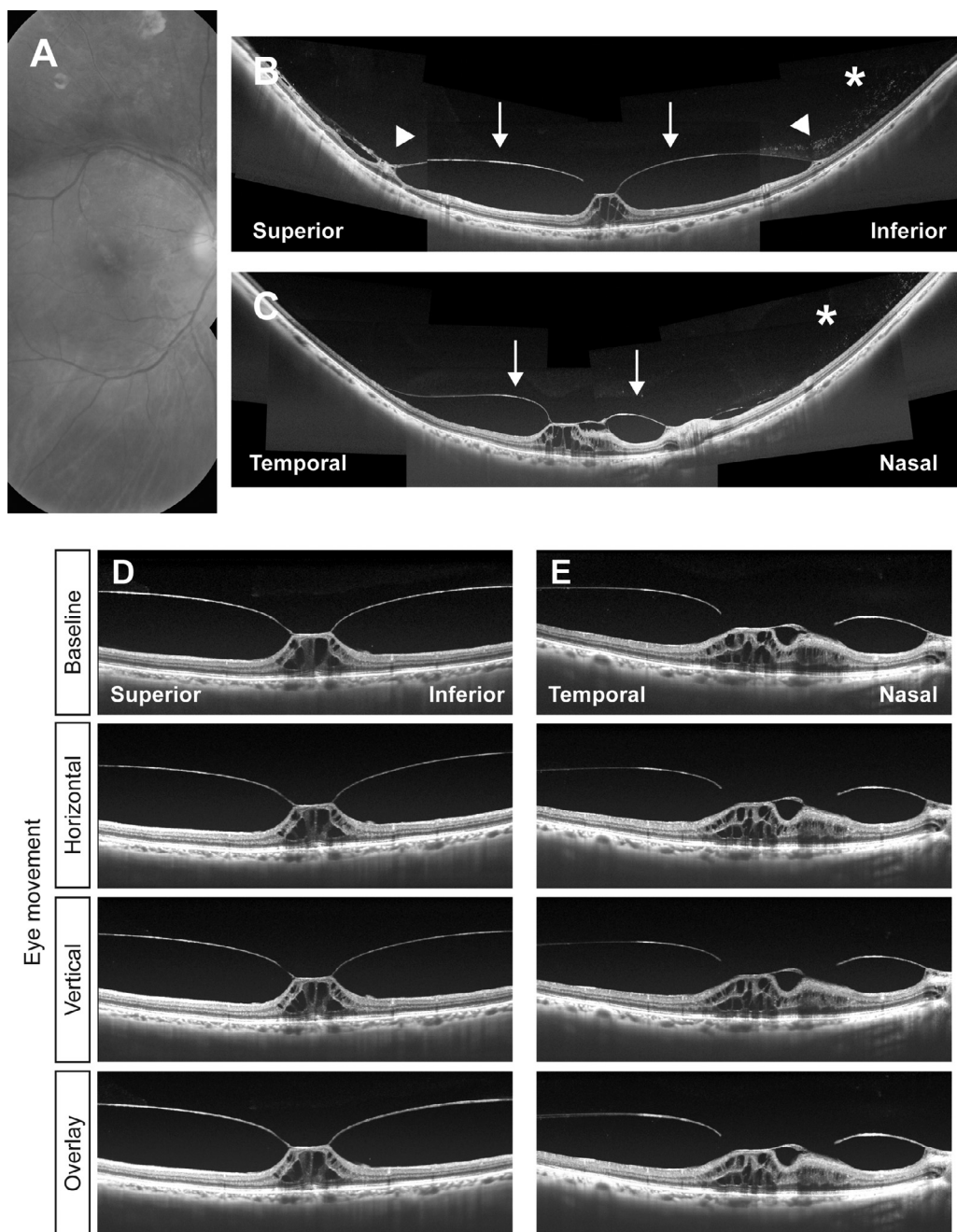


**FIGURE 1.** The fundus (A) and optical coherence tomography (OCT) images (B–E) of a 71-year-old man with a thickened posterior vitreous cortex (proliferative vitreomacular traction [VMT]). A. A vertical montaged image of the fundus demonstrating the OCT scanned range. B, C. The montaged wide-angle OCT images show the thick posterior vitreous firmly attaches to the retina at the fovea and the optic disc. Fibrous anchors set at the boundary of posterior vitreous detachment (PVD) (*arrowheads*) and a constant taut and convex posterior vitreous (*arrows*). The fovea is elevated associated with macular deformation and retinal cysts. At the mid-periphery granular hyper-reflections are evident (*asterisks*). D, E. OCT images before and after horizontal or vertical ocular movements demonstrate that the thickened posterior vitreous hardly changes its contour and position with ocular movements.

vitreous position and multiple posterior vitreous lines in the superimposed OCT images. Dynamic motion in GIF pseudoanimations before and after an ocular motion was present (Figure 3E and F, Figure 4E and F, Supplemental Data/Videos 2 and 3, and Table 2) ( $P = 2.0 \times 10^{-8}$ ).

## DISCUSSION

In the current study, we classified VMT into 2 distinct subtypes, namely, proliferative and nonproliferative, based on

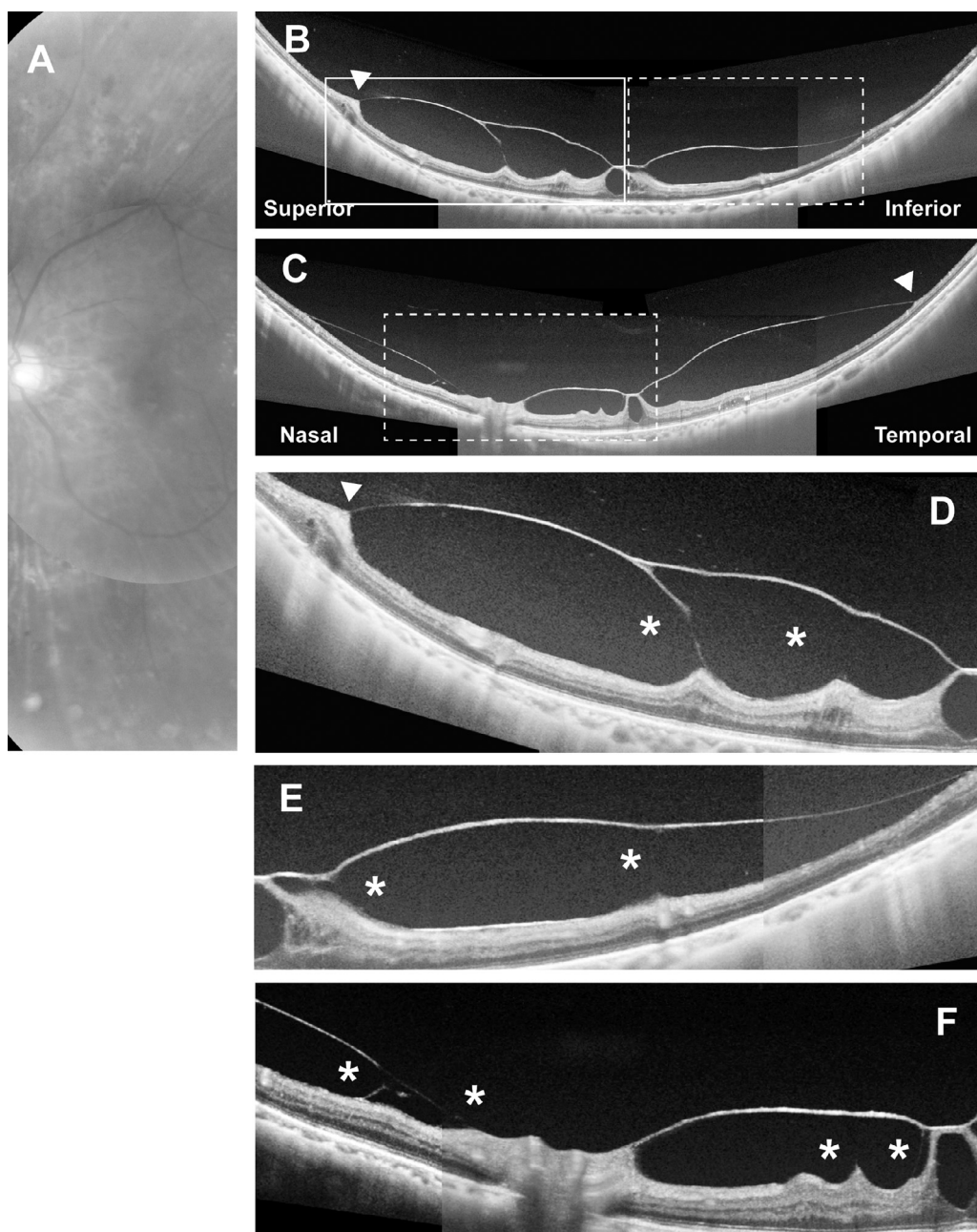


**FIGURE 2.** The montaged fundus (A) and optical coherence tomography (OCT) images (B-F) with proliferative vitreomacular traction (VMT) (a 72-year-old man). B, C. The thick posterior vitreous has a taut and convex contour and attaches to multiple points on the retina over the macula with fibrous anchors including the fovea, the optic disc and the boundary of posterior vitreous detachment (PVD) (*arrowhead*). The retina at these vitreoretinal adhesion points is elevated. D-F. Magnified images of insets in B and C (D, solid line rectangle in B; E, dotted line rectangle in B; F, dotted line rectangle in C). Note that the epiretinal membrane (ERM) and the thickened posterior vitreous are joined with the pillar-like structures (\*) and create multiple cysts over the macula.

the morphological characteristic of the posterior cortical vitreous. In eyes with nonproliferative VMT, the posterior vitreous is flexible and mobile with eye motion. The more mobile vitreous implicates a dynamic VMT resulting from ocular saccades as the primary pathomechanism of the macular pathology seen in this subtype of VMT. In the second subtype, proliferative VMT, patients have a static, thickened, and taut posterior vitreous. The static

contractile forces of the thickened posterior vitreous at the macula may also be mechanistically significant with regard to resulting macular pathology. In eyes with proliferative VMT, pathological alterations occurred predominantly in the macula and paramacular region. These alterations were characterized by points of strong vitreoretinal adhesion at fibrous anchors that limited PVD extension anteriorly.

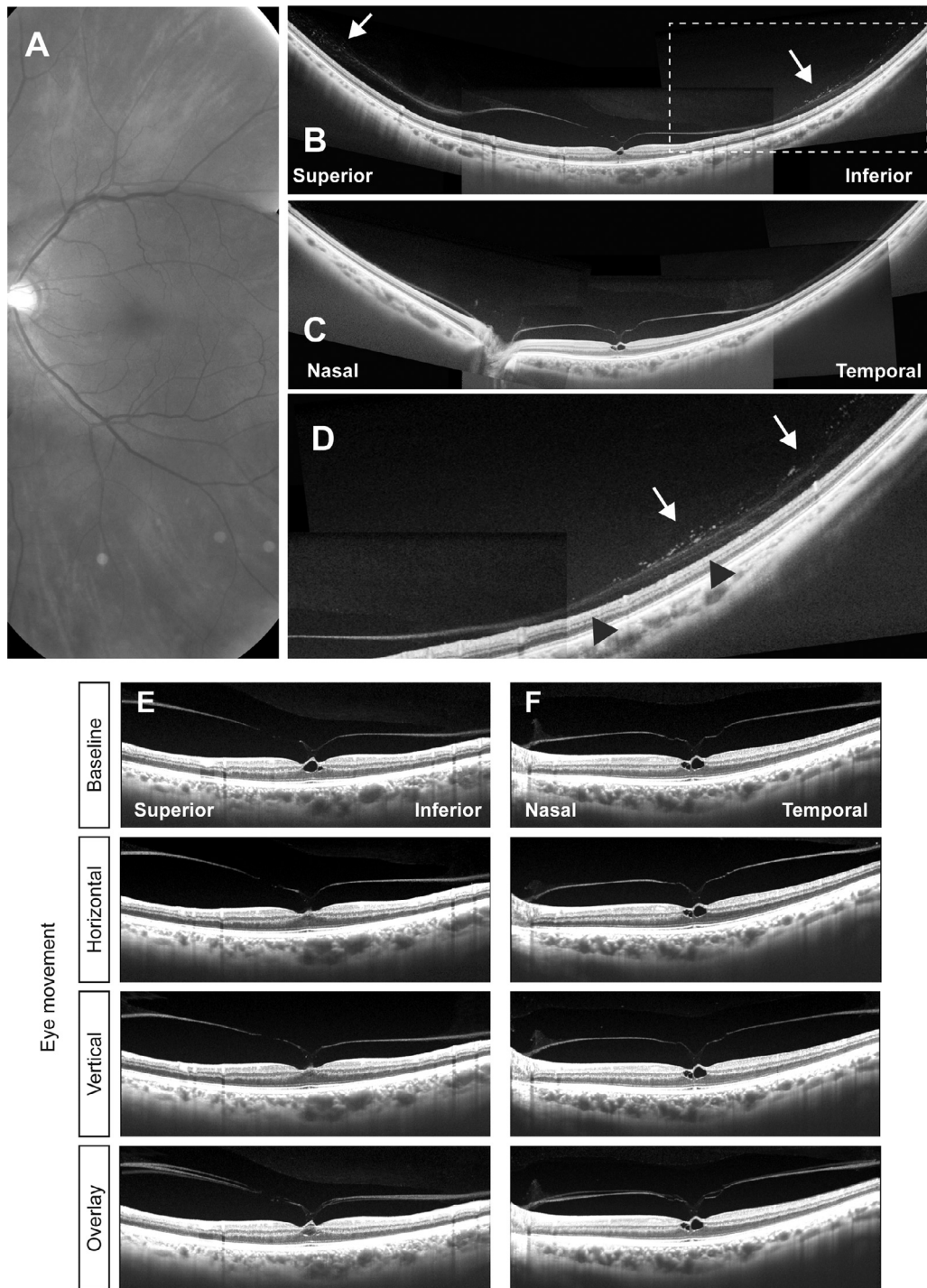


**FIGURE 3.** The fundus image (A) and OCT images (B–F) of vitreomacular traction (VMT) without thick posterior vitreous (61-year-old man, nonproliferative VMT). B, C. The montaged wide-angle optical coherence tomography (OCT) images demonstrate posterior cortical vitreous attaching to the fovea and the posterior vitreous smoothly transitions to the periphery. The fovea is elevated and shows an intraretinal cyst. Vitreoschisis and granular hyperreflections are evident in the peripheral vitreous (*arrows*). D. A magnified image of the inset in B, showing a narrow but distinct separation of the posterior vitreous from the retina expanding beyond the observable range (*arrowheads*). E, F. Overlaid OCT images of before and after horizontal or vertical ocular saccades demonstrate 3 lines of the posterior vitreous, indicating posterior vitreous changes its position after ocular movements.

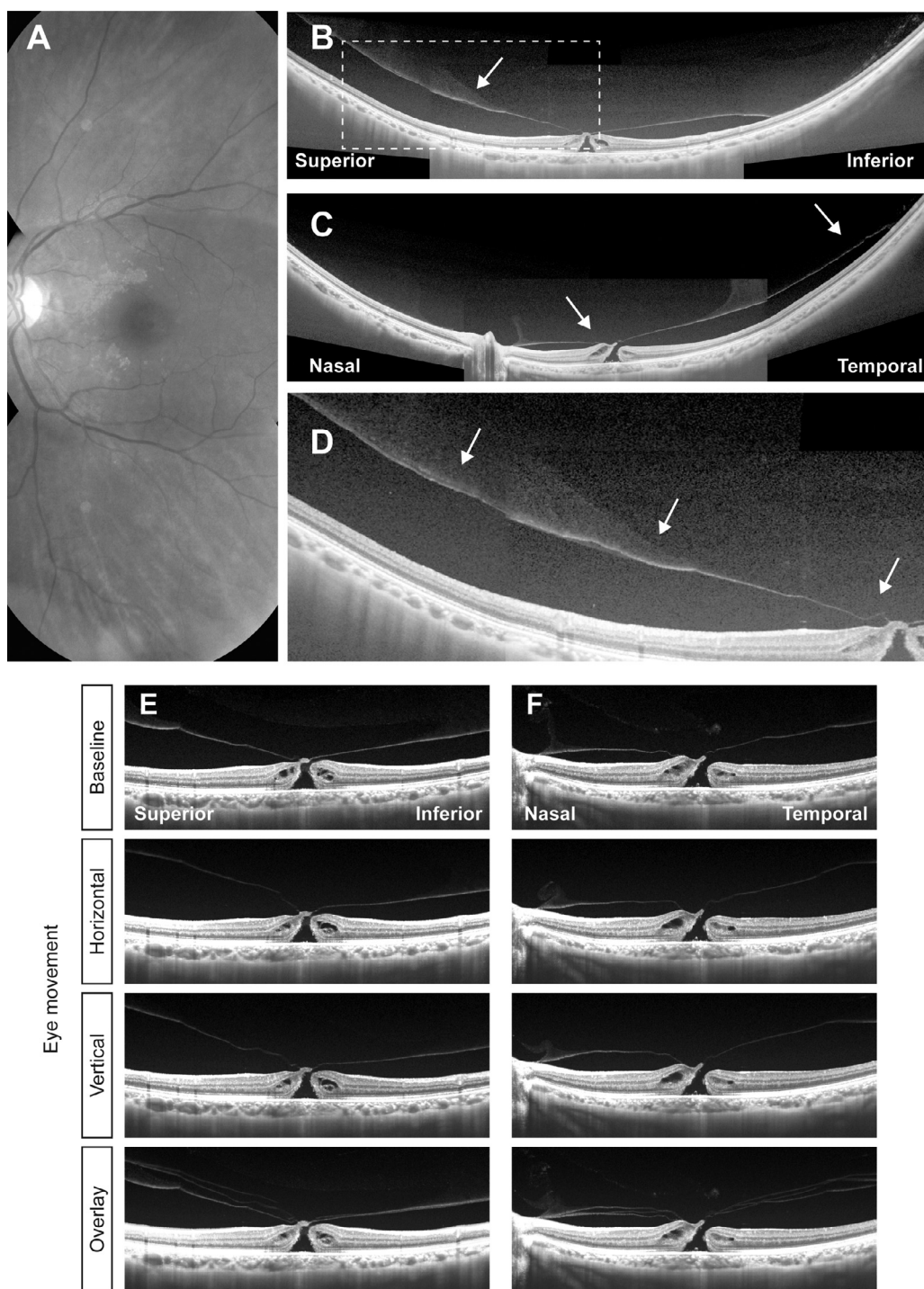


**FIGURE 4.** The fundus image (A) and optical coherence tomography (OCT) images (B–F) of nonproliferative vitreomacular traction (VMT) associated with full-thickness macular hole (70-year-old man). B, C. The posterior vitreous does not show thickening in montaged wide-angle OCT images. D. A magnified image of the inset in B. Note the wavy configuration of posterior vitreous (*arrows*) and widely extended posterior vitreous detachment (PVD) especially in the superior quadrant. E, F. The posterior vitreous has a wavy configuration, which changes the contour and position before and after the ocular movements.

The state of the posterior vitreous and its attachment to the macula has been suggested to determine the mode of tractional force applied. Johnson<sup>5,6,23</sup> has proposed that the balance between static and dynamic vitreous tractional forces in a particular eye helps determine whether VMT results in macular hole formation or a persistent macular traction disorder. In support of this hypothesis, we found that macular holes were much more commonly associated with the dynamic traction of nonproliferative VMT than with the static traction of proliferative VMT. Regarding macular hole progression, we have previously demonstrated that the dynamic posterior vitreous movements have a significant impact on anteroposterior tractional forces on the parafovea.<sup>11,12</sup> Likewise, eyes with nonproliferative VMT had a wavy-contoured posterior vitreous, which was very flexible and mobile immediately after eye motion, implicating the dynamic traction forces applied to the macula with resulting fluid currents playing potentially important pathogenetic roles. In contrast, proliferative VMT eyes did not show wavy posterior vitreous, but maintained a constantly taut and convex appearance, and the thick posterior vitreous face line did not change in contour or position during vitreous gel movement. These findings suggest that the posterior vitreous with proliferative VMT is not relaxed and that static tractional forces, generated by the persistent contraction of the convex thick posterior vitreous, may be important in the development of macular pathology. A limitation of this tracking method is the difficulty in capturing movements when an object moves substantially but returns to the original position quickly. Therefore, our data do not exclude a possible contribution by dynamic movement of the vitreous gel to the pathomechanisms in proliferative VMT. Because of the elastic nature of the posterior vitreous, it is possible that dynamic motion of the vitreous gel and fluid amplifies the sustained contractive force of the taut posterior hyaloid upon the macula.<sup>6</sup> This hypothesis may be tested by real-time observation when a high-resolution video system of OCT becomes available.

We found a concurrent ERM in almost all eyes with proliferative VMT. The ERM was integrated into taut and convex posterior vitreous with pillar-like structures and cysts,

which were distributed broadly over the macula. The probability of seeing ERM in nonproliferative VMT was comparatively much lower. Concurrence of ERM and thick posterior vitreous in VMT has been reported from intraoperative observations, 3D spectral-domain OCT and histopathological studies.<sup>6-8</sup> Although the origin of thick posterior vitreous in VMT is still debatable, the ERM and the thick posterior vitreous are connected together as a result of cellular proliferation.<sup>7,23</sup> Prior work reports that the composition of proliferative cells includes myofibroblast and fibroblast, and they create a strong anchoring between the posterior vitreous and the retina around the macula, resulting in persistent vitreoretinal traction stresses and the prevention of spontaneous vitreoretinal separation.<sup>5,6,23</sup> We found that the majority of proliferative VMT eyes were associated with fibrous anchors and that a convex and thickened posterior vitreous was distributed around the macular region, whereas posterior cortical vitreous in nonproliferative VMT was often detached beyond the observable range of wide-angle montaged OCT. No eyes with nonproliferative VMT had observable fibrous anchors. These findings support previous reports<sup>5,6,23</sup> and indicate that, in eyes with proliferative VMT, pathological alterations occur predominantly around the macular region with strong vitreoretinal adhesion at the fibrous anchors, preventing spontaneous vitreomacular separation and normal progression of PVD anteriorly.

Previous studies have classified VMT based on the area of vitreomacular attachment<sup>3,20</sup> or the V-/J-shaped pattern of the PVD.<sup>21,22</sup> The eyes with proliferative VMT showed a wider vitreomacular attachment and a higher prevalence of broad VMT as compared with those with nonproliferative VMT. We found only 4 eyes with a J-shaped pattern in this study and all were of the proliferative VMT type. Although there remains a possible association between proliferative VMT and a J-shaped pattern of PVD, these findings indicate that the width of vitreomacular attachment better reflects the characteristic of proliferative/nonproliferative VMT subtypes than it does patterns of persistent vitreous attachment. This finding may implicate a possible role of cellular proliferation facilitating increased vitreous adhesion to the macula.

---

ALL AUTHORS HAVE COMPLETED AND SUBMITTED THE ICMJE FORM FOR DISCLOSURE OF POTENTIAL CONFLICTS OF INTEREST and none were reported.

*Acknowledgments:* The authors thank Junji Kanno of Saitama Medical University and Mayuka Tsukahara of the International University of Health and Welfare for help with the technical innovation of montaged imaging.

*Funding/Support:* This research was supported in part by a grant-in-aid for scientific research (19K09998) from the Ministry of Education, Culture and Science in Japan, AMO Contracted Research Grant Program (AS2020A000025607) and a generous gift by Dr. Hiroaki Isono (KM). Research to Prevent Blindness, New York, New York, USA, and gifts by the J. Willard and Alice S. Marriott Foundation, the Gale Trust, Mr. Herb Ehlers, Mr. Bill Wilbur, Mr. and Mrs. Rajandre Shaw, Ms. Helen Nassif, Ms Mary Ellen Keck, Don and Maggie Feiner, Dick and Gretchen Nielsen, and Mr. Ronald Stiff (PLG).

*Financial Disclosures:* All authors have no financial disclosure to report.

---

## REFERENCES

1. McDonald HR, Johnson RN, Schatz H. Surgical results in the vitreomacular traction syndrome. *Ophthalmology*. 1994;101(8):1397-1403.
2. Shechtman DL, Dunbar MT. The expanding spectrum of vitreomacular traction. *Optometry*. 2009;80(12):681-687.
3. Duker JS, Kaiser PK, Binder S, et al. The International Vitreomacular Traction Study Group classification of vitreomac-

- ular adhesion, traction, and macular hole. *Ophthalmology*. 2013;120(12):2611–2619.
4. Sebag J. Vitreoschisis. *Graefes Arch Clin Exp Ophthalmol*. 2008;246(3):329–332.
  5. Johnson MW. Tractional cystoid macular edema: a subtle variant of the vitreomacular traction syndrome. *Am J Ophthalmol*. 2005;140(2):184–192.
  6. Johnson MW. Posterior vitreous detachment: evolution and complications of its early stages. *Am J Ophthalmol*. 2010;149(3):371–382.
  7. Chang LK, Fine HF, Spaide RF, Koizumi H, Grossniklaus HE. Ultrastructural correlation of spectral-domain optical coherence tomographic findings in vitreomacular traction syndrome. *Am J Ophthalmol*. 2008;146(1):121–127.
  8. Koizumi H, Spaide RF, Fisher YL, Freund KB, Klanicnik Jr JM, Yannuzzi LA. Three-dimensional evaluation of vitreomacular traction and epiretinal membrane using spectral-domain optical coherence tomography. *Am J Ophthalmol*. 2008;145(3):509–517.
  9. Bottós J, Elizalde J, Arevalo JF, Rodrigues EB, Maia M. Vitreomacular traction syndrome. *J Ophthalmic Vis Res*. 2012;7(2):148–161.
  10. Kampik A, Kenyon KR, Michels RG, Green WR, de la Cruz ZC. Epiretinal and vitreous membranes. Comparative study of 56 cases. *Arch Ophthalmol*. 1981;99(8):1445–1454.
  11. Mori K, Kanno J, Gehlbach PL, Yoneya S. Montage images of spectral-domain optical coherence tomography in eyes with idiopathic macular holes. *Ophthalmology*. 2012;119(12):2600–2608.
  12. Mori K, Gehlbach PL, Kishi S. Posterior vitreous mobility delineated by tracking of optical coherence tomography images in eyes with idiopathic macular holes. *Am J Ophthalmol*. 2015;159(6):1132–1141.
  13. Smiddy WE, Michels RG, Glaser BM, deBustros S. Vitrectomy for macular traction caused by incomplete vitreous separation. *Arch Ophthalmol*. 1988;106(5):624–628.
  14. Sadda SR, Campochiaro PA, de Juan Jr E, Haller JA, Green WR. Histopathological features of vitreous removed at macular hole surgery. *Arch Ophthalmol*. 1999;117(4):478–484.
  15. Liu JJ, Witkin AJ, Adhi M, et al. Enhanced vitreous imaging in healthy eyes using swept source optical coherence tomography. *PLoS One*. 2014;9(7):e102950.
  16. Li D, Kishi S, Itakura H, Ikeda F, Akiyama H. Posterior precortical vitreous pockets and connecting channels in children on swept-source optical coherence tomography. *Invest Ophthalmol Vis Sci*. 2014;55(4):2412–2416.
  17. Lavinsky F, Lavinsky D. Novel perspectives on swept-source optical coherence tomography. *Int J Retina Vitreous*. 2016;2:25.
  18. Mori K, Kanno J, Gehlbach PL. Retinochoroidal morphology described by wide-field montage imaging of spectral domain optical coherence tomography. *Retina*. 2016;36(2):375–384.
  19. Tsukahara M, Mori K, Gehlbach PL, Mori K. Posterior vitreous detachment as observed by wide-angle OCT imaging. *Ophthalmology*. 2018;125(9):1372–1383.
  20. Bottós J, Elizalde J, Rodrigues EB, Farah M, Maia M. Classifications of vitreomacular traction syndrome: diameter vs morphology. *Eye (Lond)*. 2014;28(9):1107–1112.
  21. Yamada N, Kishi S. Tomographic features and surgical outcomes of vitreomacular traction syndrome. *Am J Ophthalmol*. 2005;139(1):112–117.
  22. Sonmez K, Capone Jr A, Trese MT, Williams GA. Vitreomacular traction syndrome: impact of anatomical configuration on anatomical and visual outcomes. *Retina*. 2008;28(9):1207–1214.
  23. Johnson MW. Perifoveal vitreous detachment and its macular complications. *Trans Am Ophthalmol Soc*. 2005;103:537–567.